Hindawi
Advances in Civil Engineering
Volume 2018, Article ID 6986047, 13 pages
https://doi.org/10.1155/2018/6986047

Research Article

Low-Cycle Flexural Fatigue Behavior of Concrete Beam Reinforced with Hybrid FRP-Steel Rebar

Jinkyo F. Choo,[1] **Young-Cheol Choi**,[2] **Seung-Jun Kwon**,[3] **Ki-Tae Park**,[4] **and Sung-Won Yoo**[2]

[1]*Department of Energy Engineering, Konkuk University, 120 Neungdong-ro, Gwangjin-gu, Seoul 05029, Republic of Korea*
[2]*Department of Civil and Environmental Engineering, Gachon University, 1342 Seongnamdaero, Sujeong-gu, Seongnam-si, Gyeonggi-do 13120, Republic of Korea*
[3]*Department of Civil and Environmental Engineering, Hannam University, 70 Hannamro, Daedeok-gu, Daejeon 34430, Republic of Korea*
[4]*Structural Engineering Research Institute, Korea Institute of Civil Engineering and Building Technology, 283 Goyangdae-ro, Ilsanseo-gu, Goyang-si, Gyeonggi-do 10223, Republic of Korea*

Correspondence should be addressed to Sung-Won Yoo; imysw@gachon.ac.kr

Received 10 August 2018; Revised 10 October 2018; Accepted 18 October 2018; Published 4 November 2018

Academic Editor: Farhad Aslani

Studies examined experimentally the flexural behavior of concrete beams reinforced with the hybrid FRP-steel rebar but very few among them evaluated their fatigue performance. In this study, the fatigue test has been performed, and an analytical model for simulating the flexural fatigue behavior of the concrete beam reinforced with the hybrid bar considering its postyielding behavior is developed. A formula relating the postyielding fatigue strain of the rebar to the number of the fatigue cycle is suggested and used in the proposed procedure. The method simulating the low-cycle behavior of the reinforced concrete beam is found to be satisfactory and can predict the number of cyclic loading to failure.

1. Introduction

Reinforced concrete (RC) is a composite material in which reinforcement having higher tensile strength or ductility is included in concrete to supplement its low tensile strength and brittleness. The reinforcement is usually a steel bar which makes it prone to corrosion generated by the inevitable attack of harmful substances like chloride ions. This corrosion is a major cause of the loss of durability and structural problems encountered in RC structures [1–4].

Numerous studies were conducted to prevent the rebar corrosion caused by the ingress of chloride ions. Among them, several studies improved the resistance to chloride penetration of the concrete material by the addition of cementitious materials such as fly ash and ground-granulated blast-furnace slag. Other studies used FRP (fiber-reinforced polymer) rebar or anticorrosive steel rebar using diverse protection techniques such as galvanization, electrodeposition of seawater, or epoxy coating [5–7]. However, FRP material is brittle with a low modulus of elasticity despite of a very high durability [8]. Later, some researchers proposed to use the hybrid FRP-steel rebar [9]. The hybrid FRP-steel bar is the monolithic combination of a FRP skin braided around the steel rebar to take full advantage of the elastic modulus of steel and the high durability of FRP. A lot of researches reported that the hybrid FRP-steel bar has a higher chloride resistance than the conventional steel bar and that the bond strength with concrete using the hybrid bar reaches at least 80% of that developed by the conventional steel bar [10–14]. Especially, the combination of FRP and steel achieves enhanced postyielding behavior. Meanwhile, Kara et al. [15] predicted numerically the flexural behavior of hybrid FRP-steel RC beams. Sun et al. [16] reported that most of the studies dedicated to the hybrid-reinforced concrete beam focused on the corrosion control and stiffness improvement and investigated the mechanical properties of the hybrid rebar under tensile, repeated tensile, and compressive loading.

The fatigue problem in RC beams has also been dealt in numerous studies [17–21]. Fatigue generally occurs through the repeated action of the live loads and may lead to failure below the yield strength of steel. This phenomenon is influenced by the number of loading cycles and the size of the fatigue load. Recently, research focused particularly on the fatigue behavior of RC beams strengthened with FRP [18, 19]. Some studies also examined the fatigue flexural behavior of corroded RC beams strengthened with FRP sheets [20, 21]. Sun et al. [16] evaluated the behavior of the hybrid rebar subjected to cyclic tensile loading and stressed the role of the postyielding stiffness of the rebar owing to the combination of the linear elastic FRP and the elastic-plastic steel bar. Harris et al. [22] also examined experimentally the cyclic behavior of the hybrid FRP-steel bar, and Won et al. [23] evaluated the durability of the hybrid FRP-steel bar exposed to marine environment. In concern with the beam reinforced with the hybrid FRP-steel bar, Sim et al. [24] conducted an experimental study on the fatigue flexural characteristics of concrete beams reinforced with the FRP rebar and hybrid steel-FRP rebar. These authors reported that the fatigue strength after 2 million cycles of the RC structure using the steel rebar dropped down to about 65% of the static ultimate strength and that the RC structure using the hybrid rebar should be examined under fatigue because apart from the number of loading cycles and the size of the fatigue load, the material characteristics of the rebar play a critical role in the fatigue behavior [24]. Hwang et al. [25] investigated experimentally the mechanical performance of RC beams reinforced with the hybrid rebar under cyclic loading. Confirming previous research results, it was concluded that the RC beam reinforced with the hybrid rebar developed smaller crack width, scattered crack pattern, and higher elastic recovery than the conventional RC beam. However, considering that the corrosion of the rebar is resolved to some extent, it is noteworthy that there are still very few studies predicting analytically the long-term performance like the fatigue behavior, since fatigue may represent one major problem that will be faced by the beam reinforced with the hybrid FRP-steel rebar.

Accordingly, the present study intends to further the work of Hwang et al. [25] by proposing an analytical model predicting the low-cycle flexural fatigue behavior of the concrete beam reinforced with the hybrid FRP-steel bar. To that goal, two sets of concrete beam specimens reinforced with the hybrid FRP-steel rebar and the conventional steel rebar were fabricated. The first set of beams was subjected to the static test up to failure, and the fatigue test at the low cycle was conducted on the second set of beams for the evaluation of the fatigue performance. The test results are used to establish a general formula relating the postyielding fatigue strain of the rebar to the number of the fatigue cycle. Using this formula, an analytical procedure is then proposed based upon the strain compatibility condition to predict the low-cycle flexural fatigue behavior of the RC beam.

2. Materials

2.1. Concrete. Table 1 gives the mix proportions of the concrete used for all the specimens in this study. The target strength of concrete was 24 MPa, and the evaluation of the compressive strength on specimens gave a slightly higher value of 25.3 MPa.

2.2. Steel Rebar and Hybrid FRP-Steel Rebar. As mentioned in the introduction, FRP rebar was considered as a solution to overcome the corrosion problem of the steel rebar. Even though the FRP rebar provides outstanding features like noncorrosiveness, high tensile strength, fatigue resistance, lightweight, nonmagnetism, nonconductivity, and easy treatment, its low modulus of elasticity, brittleness in failure, and high cost refrains its exploitation on-site [12]. Therefore, the concept of the hybrid FRP-steel rebar (FRP hybrid rebar) was introduced to compensate these drawbacks. The hybrid FRP-steel bar is the monolithic combination of a FRP skin braided around the steel rebar to take full advantage of the elastic modulus of steel and the high durability of FRP [11].

In this study, the adopted hybrid FRP-steel bar shown in Figure 1 is the glass FRP (GFRP) rebar that was developed by the Korea Institute of Construction and Building Technology (KICT). The core of the rebar is a deformed steel bar over which the GFRP skin is braided [11, 12, 24, 25].

Concurrently to the hybrid FRP-steel rebar, conventional steel rebar was also considered for comparison. The specifications of both types of the rebar adopted in this study are listed in Table 2. Note that the deformed D13 bar was used as steel rebar, and that the hybrid FRP-steel rebar has a core D9 steel bar wrapped by GFRP to achieve the D13 rebar. The tensile strength test was conducted on the rebars to determine their material properties. The measurement of the tensile strength test is plotted in Figure 2. The corresponding values of the yield strength and tensile modulus are, respectively, 475 MPa and 200 GPa for the steel rebar and 330 MPa and 92 GPa for the hybrid rebar.

3. Static and Fatigue Tests of the RC Beam

For the tests, two sets of RC beams were fabricated using the concrete mix of Table 1 reinforced with the rebars of Table 2 as stirrups and tensile reinforcement. The 4 beam specimens have dimensions of 2,175 × 200 × 200 mm with a span length of 1,800 mm between the supports. Figure 3 shows the cross section of the beams in which the reinforcement is arranged in the tension and shear zones. As shown in Figure 4, thirteen D13 stirrups were disposed at a spacing of 150 mm with two D13 stirrups distant by 100 mm from these central stirrups and along 2,000 mm of the specimens. For the measurement in both static and fatigue tests, 2 rebar strain gages were installed at the center of each of the two longitudinal rebars. LVDTs (linear variable displacement transducer) with a stroke of 100 mm were also mounted at the midspan and at 300 mm from the midspan (at $L/3$) to measure the deflection [25].

3.1. Static Test. The static test was first performed on the first set of beam specimens prior to the evaluation of the fatigue behavior. The three-point bending test was conducted using a hydraulic actuator (MTS) with a capacity of 2,000 kN (Figure 5).

Table 1: Mix proportions of concrete used in this study.

W/B (%)	S/a (%)	Maximum aggregate size (mm)	Slump (mm)	Unit weight (kg/m^3)				AE (kg/m^3)
				Water	Cement	Sand	Aggregates	
50	50	25	180	175	353	888	902	2.47

Figure 1: Hybrid GFRP-steel rebar developed by KICT [12].

Table 2: Specifications of hybrid FRP-steel rebar and steel rebar used in this study.

Rebar type	Diameter	f_y (MPa)	f_u (MPa)	ε_y	ε_u	E_s (MPa)
Steel	D13	475	589.2	0.00238	0.201	2.00×10^5
Hybrid steel-FRP	D13	330	777.7	0.00359	0.370	0.92×10^5

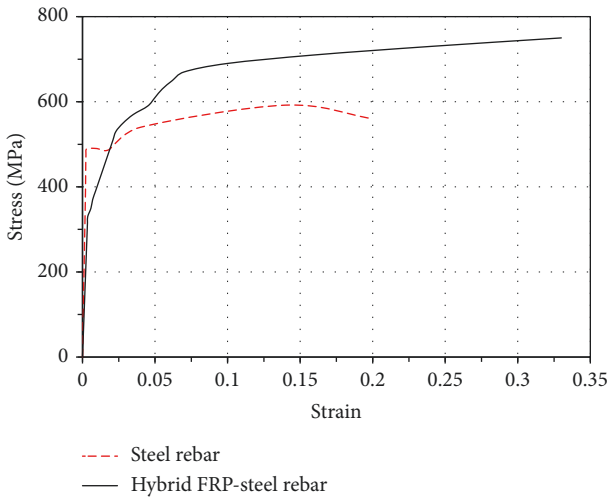

Figure 2: Tensile strength test results of hybrid FRP-steel rebar and steel rebar used in this study.

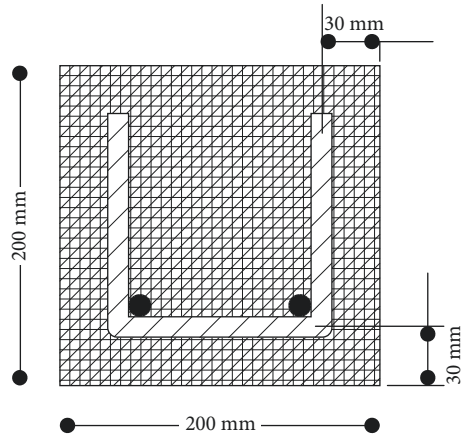

Figure 3: Cross section of RC beam specimens reinforced by steel and hybrid rebars used in this study.

Table 3 arranges the static test results for the RC beam specimens reinforced by conventional D13 steel rebars (RC-SR) and RC beam specimens reinforced by D13 hybrid FRP-steel rebars (RC-HR). In Table 3, P_y, δ_y, P_u, and δ_u denote the yield and ultimate loads and displacements, respectively. The measured load-deflection curve, load-tensile strain of the rebar, and load-compressive strain of concrete at mid-span are plotted in Figure 6.

As indicated in Table 3, the yield load was attained at 36.0 kN for RC-HR and 48.9 kN for RC-SR. Owing to the strengthening action of the hybrid FRP-steel rebar, the final failure load of RC-HR increased to reach the value of 50.0 kN equal to that of RC-SR.

In view of Figure 6, the deflection at midspan of RC-SR reached 7.6 mm at yielding and became 22.2 mm at failure. For RC-HR, this value was 11.3 mm at yielding and reached 25.0 mm at failure by brittle rupture. The deflection measured by the LVDTs installed at midspan and at 300 mm far from midspan (L/3) gave respective values of 6.8 mm and 16.5 mm at the yield and failure of RC-SR. For RC-HR, the deflection at this point was 9.0 mm at yielding and, after yielding of the rebar, the beam exhibited linear behavior enabling it to sustain larger load through the clear occurrence of tension hardening. Both types of RC beams showed similar cracking loads with 6.0 kN for RC-SR and 5.5 kN for RC-HR. In concern with the strain in the longitudinal reinforcement, the yield strength ranged around 2,500 $\mu\varepsilon$ for RC-SR and 3,600 $\mu\varepsilon$ for RC-HR after which linear behavior

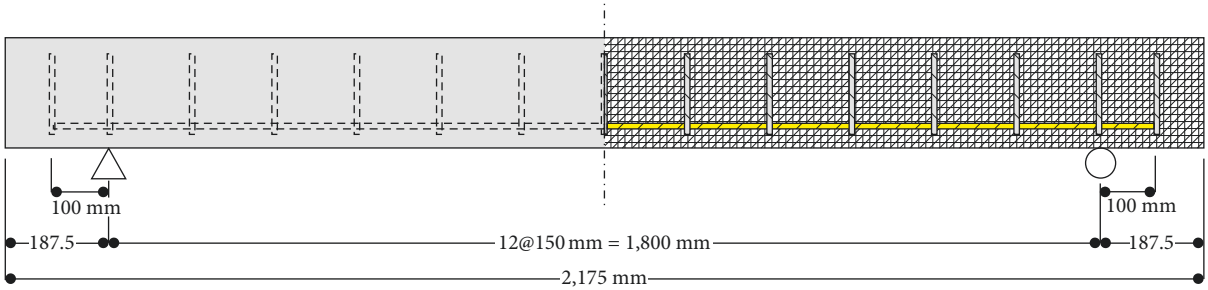

Figure 4: Arrangement of longitudinal reinforcement and stirrups in RC beams used in this study [25].

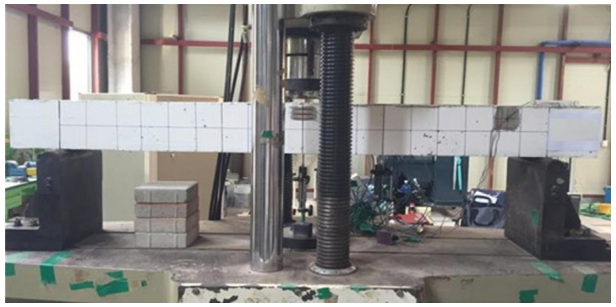

Figure 5: Static test of the RC beam specimen [25].

Table 3: Static test results of RC beams.

RC beam specimen	Yield		Ultimate	
	P_y (kN)	δ_y (mm)	P_u (kN)	δ_u (mm)
RC-SR	48.9	8.6	50.0	22.2
RC-HR	36.0	11.3	50.0	25.0

with tension hardening could be observed as reported by Hwang et al. [25].

Figure 7 shows the crack patterns observed in the specimens after the static test. The cracks in RC-SR are seen to develop narrower than in RC-HR for the considered beams, but one cannot draw general conclusions due to the limited number of specimens involved in the test.

3.2. Fatigue Test. Based upon the static test results, the fatigue load to be applied on the RC beams was set to maximum 0.85 P_y and minimum 0 kN with a frequency of 1 Hz. Specifically, the maximum fatigue load was 41.6 kN for RC-SR and 30.6 kN for RC-HR. The RC beam specimens were subjected to 100 cycles of fatigue loading after the yield of the reinforcement followed by static loading up to failure. The setup of the fatigue test was identical to that of the static test shown in Figure 5.

It is known that the loss of bond performance results generally in the reduction of the number of cracks. This observation was partially verified in the static test results. Figure 8 shows the crack patterns observed in all the specimens after the fatigue test. Similarly to the static test, RC-SR showed numerous cracks with narrow spacing, whereas RC-HR presented relatively larger spacing between the cracks. Figure 9 compares the results of the fatigue test for RC-SR and RC-HR. RC-HR exhibited better restoring force than RC-SR in terms of the recovery of the deflection after the removal of the fatigue load.

4. Proposed Formula for Postyielding Fatigue Strain of the Rebar

The load-rebar strain curves of Figure 9 measured during the fatigue test of the RC beam specimens were analyzed statistically using the predictive analysis software SPSS (Statistical Package for the Social Sciences) to derive the relation between the number of loading cycles and the rebar strain, as expressed in the following equation:

$$\varepsilon_{s,f} = \frac{\varepsilon_y - \varepsilon_{si}}{\varepsilon_{si} - 373 \times \log_{10} N}, \tag{1}$$

where $\varepsilon_{s,f}$ is the postyielding rebar strain due to fatigue load, ε_y is the yield strain of rebar, ε_{si} is the static strain under the maximum cyclic load, and N is the number of loading cycles.

The value of 373 in the denominator of Equation (1) corresponds to the arithmetic mean of 371 and 375 obtained for RC-SR and RC-HR, respectively. Since both values were similar, using the arithmetic mean seemed to be reasonable. The validity of this choice is confirmed by the values of the correlation coefficient (R^2), which is 0.8212 for RC-SR and 0.7666 for RC-HR, as shown in Figure 10.

5. Analytical Model for Predicting the Low-Cycle Fatigue Behavior of the RC Beams

This section presents the process proposed to establish the analytical model predicting the low-cycle fatigue behavior of the RC beams using the formula for the postyielding fatigue strain of the rebar in Equation (1). Since the process is based on the strain compatibility and adopts the well-known stress-strain nonlinear model of Hognestad for concrete, this model expressed in Equation (2) is presented first [26]:

$$f_c = f'_c\left(\frac{2\varepsilon}{\varepsilon_0} - \left(\frac{\varepsilon}{\varepsilon_0}\right)^2\right) \quad \text{for } \varepsilon_c \le \varepsilon_0,$$
$$f_c = f'_c\left(1 - 0.15\frac{\varepsilon_c - \varepsilon_0}{0.0038 - \varepsilon_0}\right) \quad \text{for } \varepsilon_c > \varepsilon_0, \tag{2}$$

where f_c is the concrete stress, ε is the concrete strain corresponding to f_c, f'_c is the peak concrete stress (MPa),

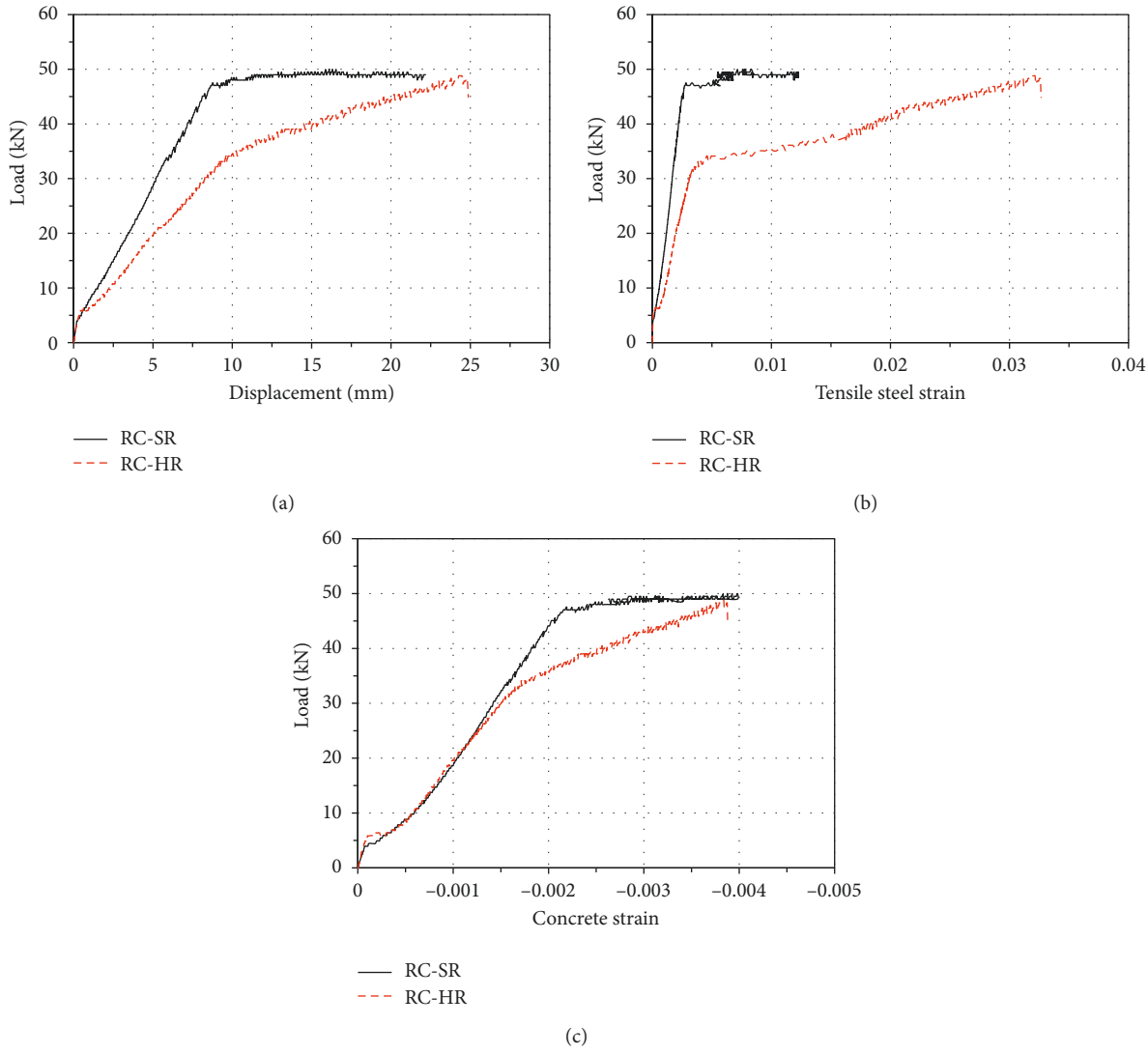

Figure 6: Comparison of static test results of RC beam specimens reinforced by the steel rebar (RC-SR) and by the hybrid FRP-steel rebar (RC-HR): (a) load-deflection curves measured at midspan [25]; (b) load-tensile strain curves measured in longitudinal reinforcement; (c) load-concrete compressive strain curves.

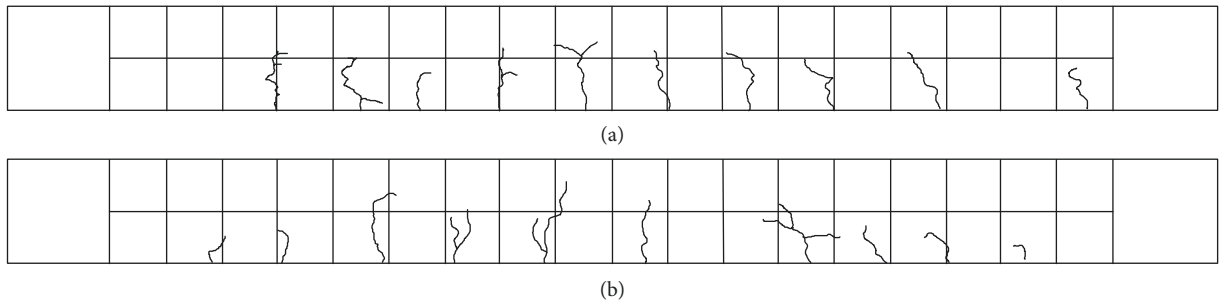

Figure 7: Crack patterns observed in RC beam specimens after the static test: (a) RC-SR; (b) RC-HR.

$\varepsilon_0 = 2f'_c/E_c$ is the ultimate strain or strain corresponding to f'_c, and E_c is the initial elastic modulus of concrete (MPa).

Considering the strain compatibility conditions, the strain in the compressive zone of the section is increased stepwise, and the corresponding stresses in steel and concrete, the flexural strength, the curvature, and the deflection are computed at each step. For the reinforced concrete cross section of height h and width b shown in Figure 11, the strain of the tensile steel (ε_s) can be determined iteratively through equilibrium by assuming the

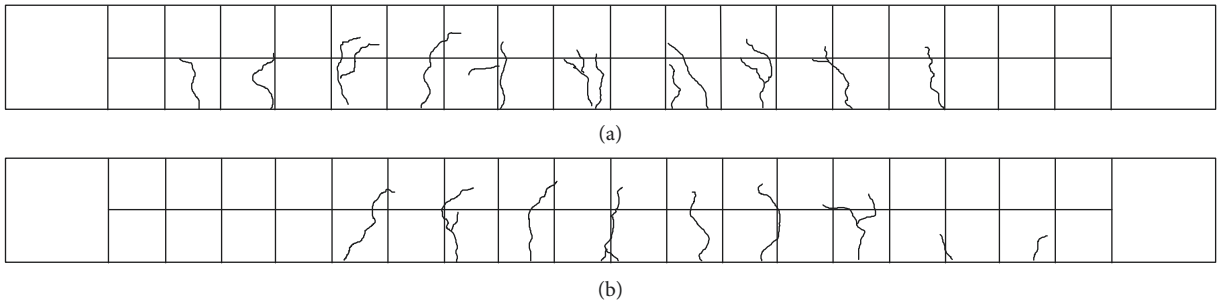

Figure 8: Crack patterns observed in RC beam specimens after the fatigue test: (a) RC-SR; (b) RC-HR.

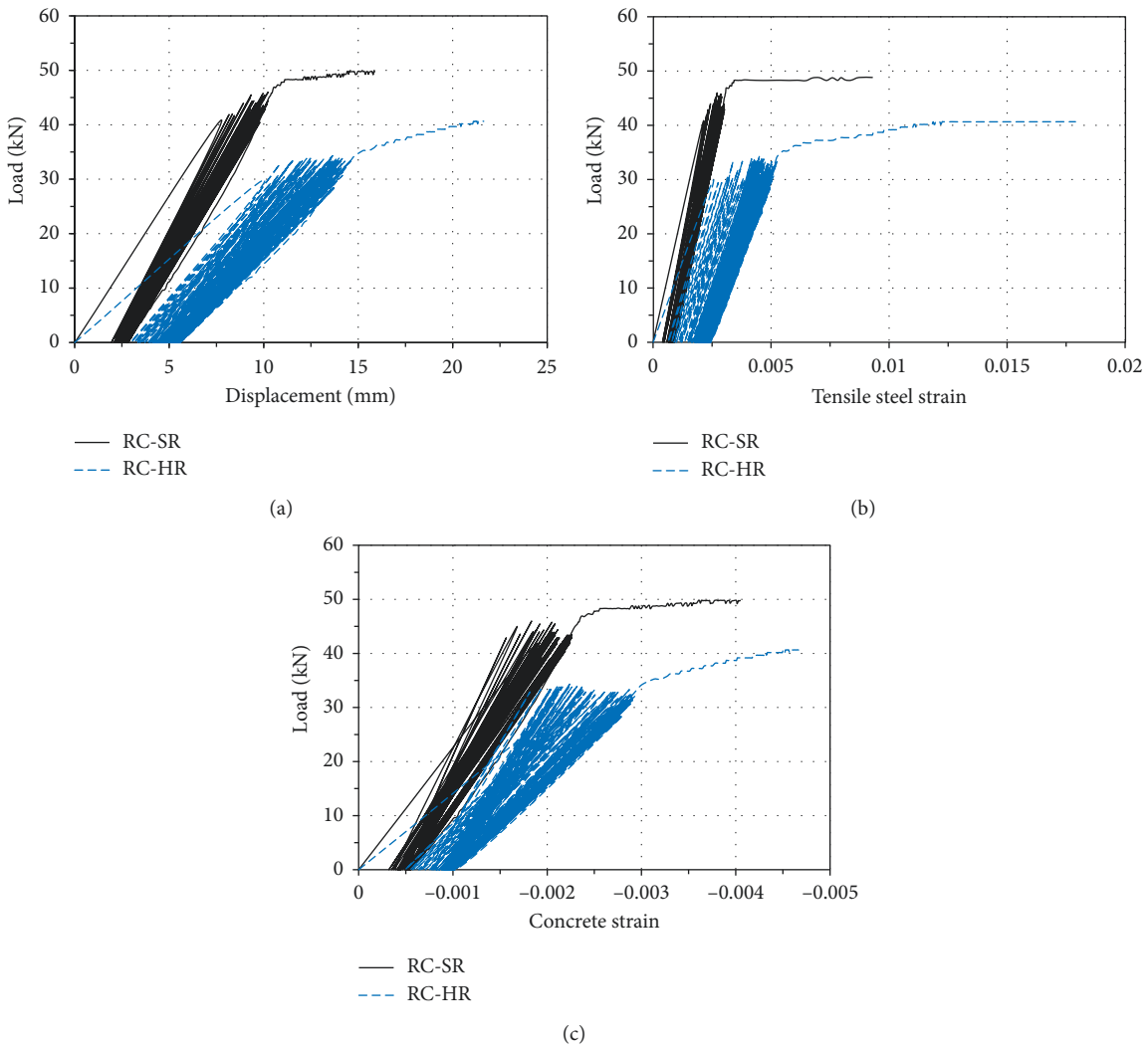

Figure 9: Comparison of fatigue test results of RC beam specimens reinforced by the steel rebar (RC-SR) and by the hybrid FRP-steel rebar (RC-HR): (a) fatigue load-deflection curves measured at midspan [25]; (b) fatigue load-tensile strain curves measured in longitudinal reinforcement; (c) fatigue load-concrete compressive strain curves.

strain at the top of the compressive zone and the strain at the bottom of concrete as follows [27]. Note that, in Figure 11, γ is a ratio expressing the position of the compressive force C_c in the compressive zone with respect to the position of the neutral axis (c), and ε_{cr} is the crack strain of concrete:

$$\begin{aligned} \varepsilon_{top} &= c\phi, \\ \varepsilon_{bottom} &= (h-c)\phi, \end{aligned} \tag{3}$$

where ϕ is the curvature, h is the height of the section, and c is the distance of the neutral axis from the top of section.

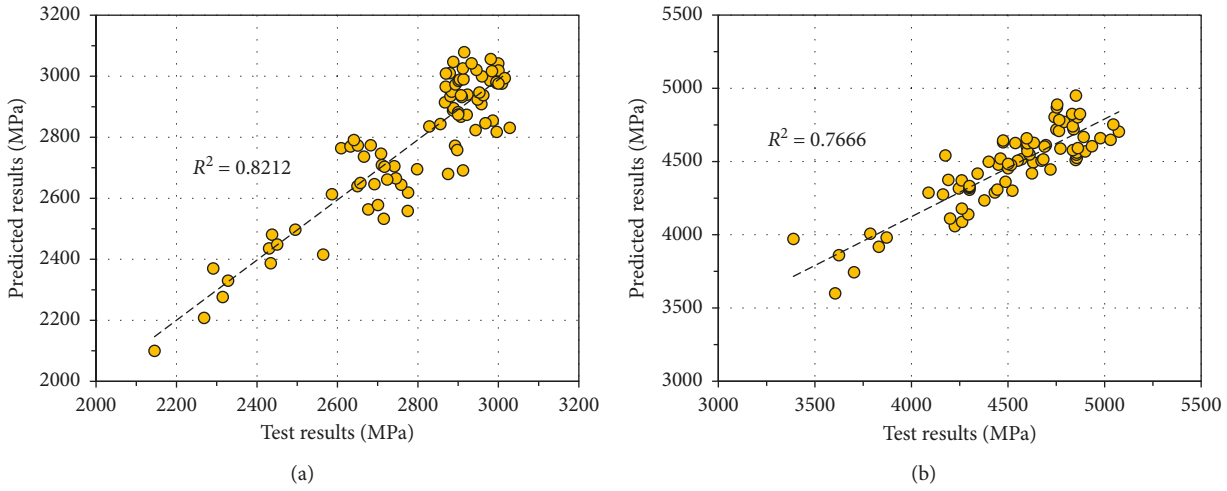

FIGURE 10: Correlation analysis of the proposed formula for postyielding fatigue strain of the rebar: (a) correlation between experimental and predicted rebar strains for RC-SR; (b) correlation between experimental and predicted rebar strains for RC-HR.

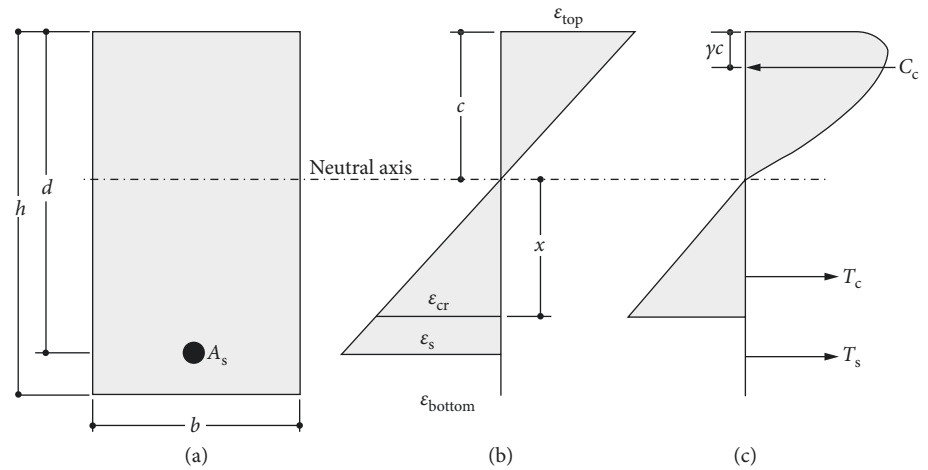

FIGURE 11: Strain compatibility of RC beam cross section for analysis [27]: (a) cross section; (b) strain distribution; (c) stress distribution.

The deformation at the top and bottom of the section can then be determined using the curvature and the depth of the neutral axis. Since the curvature expresses the change in the slope per unit length of the member, it is assumed to be equal to the slope of the strain in the cross section. The curvature in the cross section is increased by a constant increment at each analysis step. Moreover, the position of the neutral axis is assumed for each curvature to compute the strain distribution in the cross section. The strains at the top and bottom of the beam section are expressed as follows by means of the force equilibrium:

$$C_c + T_c + T_s = 0, \tag{4a}$$

$$\int_{A_c} \sigma_c \, dA_c + \int_{A_s} \sigma_s \, dA_s = 0, \tag{4b}$$

where C_c and T_c are, respectively, the compressive force and tensile force sustained by concrete; T_s is the tensile force sustained by the steel reinforcement; σ_c and σ_s are the stresses in concrete and steel, respectively; A_c is the area of concrete; and A_s is the amount of reinforcement.

The section force, that is, the moment, can be computed based upon the stress distribution within the section satisfying the force equilibrium:

$$M = \int_{A_c} \sigma_c y \, dA_c + \int_{A_s} \sigma_s y \, dA_s. \tag{5}$$

Using the following equations relating the curvature ϕ and the moment M obtained by Equation (6) gives the deflection δ developed in the member with span length L subjected to the load P at its center:

$$\theta = \arcsin\left(\frac{1}{2} L\phi\right),$$

$$\delta = \frac{1 - \cos\theta}{\phi}, \tag{6}$$

$$P = \frac{4M}{L}.$$

Figure 12 presents the flowchart of the iterative process proposed for the fatigue analysis of the reinforced beam

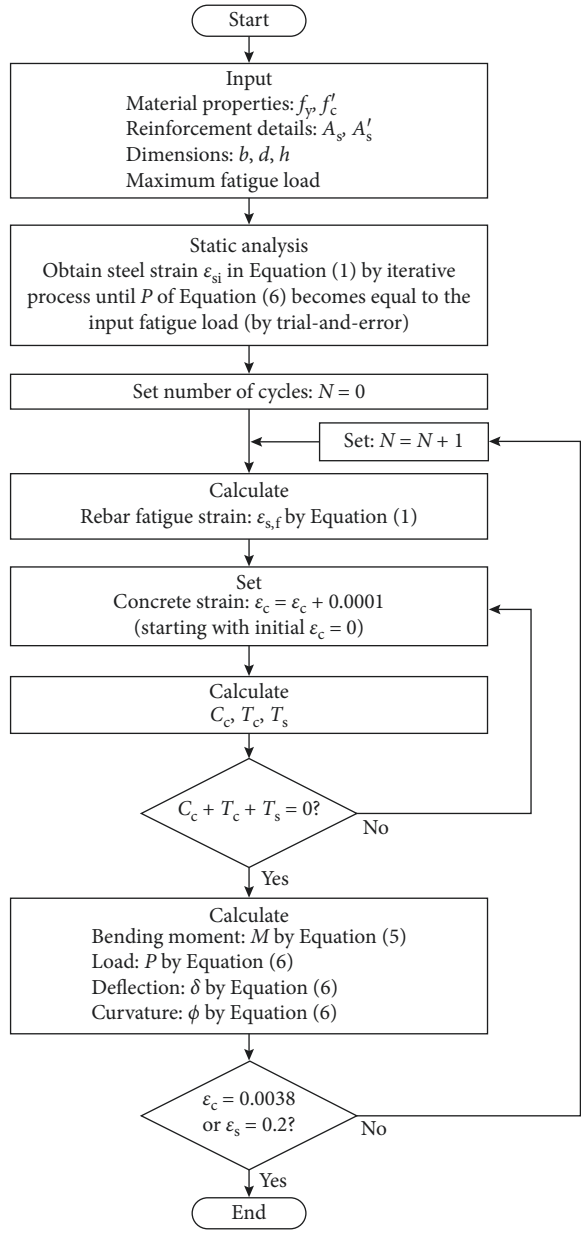

Figure 12: Flowchart of fatigue analysis for nonlinear flexural behavior of the RC beam.

including the static analysis performed to obtain the initial values to be used in the fatigue analysis. This process allows the nonlinear analysis to consider the accumulation of fatigue strain in the rebar of the RC member throughout the cyclic loading. The symbols used in Figure 12 are those defined in Figure 11 and in Equations (1)–(6).

6. Comparison of Analytical and Experimental Results

6.1. Static Behavior. Figure 13 compares the predicted and experimental flexural behaviors of the considered RC beam specimens (RC-SR; RC-HR). The predicted value of the static flexural behavior is obtained by the process depicted in Figure 12, and the experimental values are those presented in Figure 6 of Section 3.1. Note that the bilinear model was adopted for the tensile reinforcement in the analytical model.

The predicted values produced by the static analysis process proposed by Yoo et al. [27] are seen to be in good agreement with the experimental results. For the load-concrete strain curves plotted in Figure 13(c), the analysis fits accurately the experimental results until cracking, but the postcracking strain of the analysis is seen to deviate from the test data. This difference can be explained by the difference between Hognestad's model adopted in the analysis and the measured stress-strain curves of concrete. Specifically, the elastic modulus of the concrete used in the test is lower than that of Hognestad's model, but the ultimate strains of the analysis and experiment are similar. These factors also resulted in the relatively smaller rebar strain and deflection produced by the analysis of RC-HR in Figures 13(a) and 13(b).

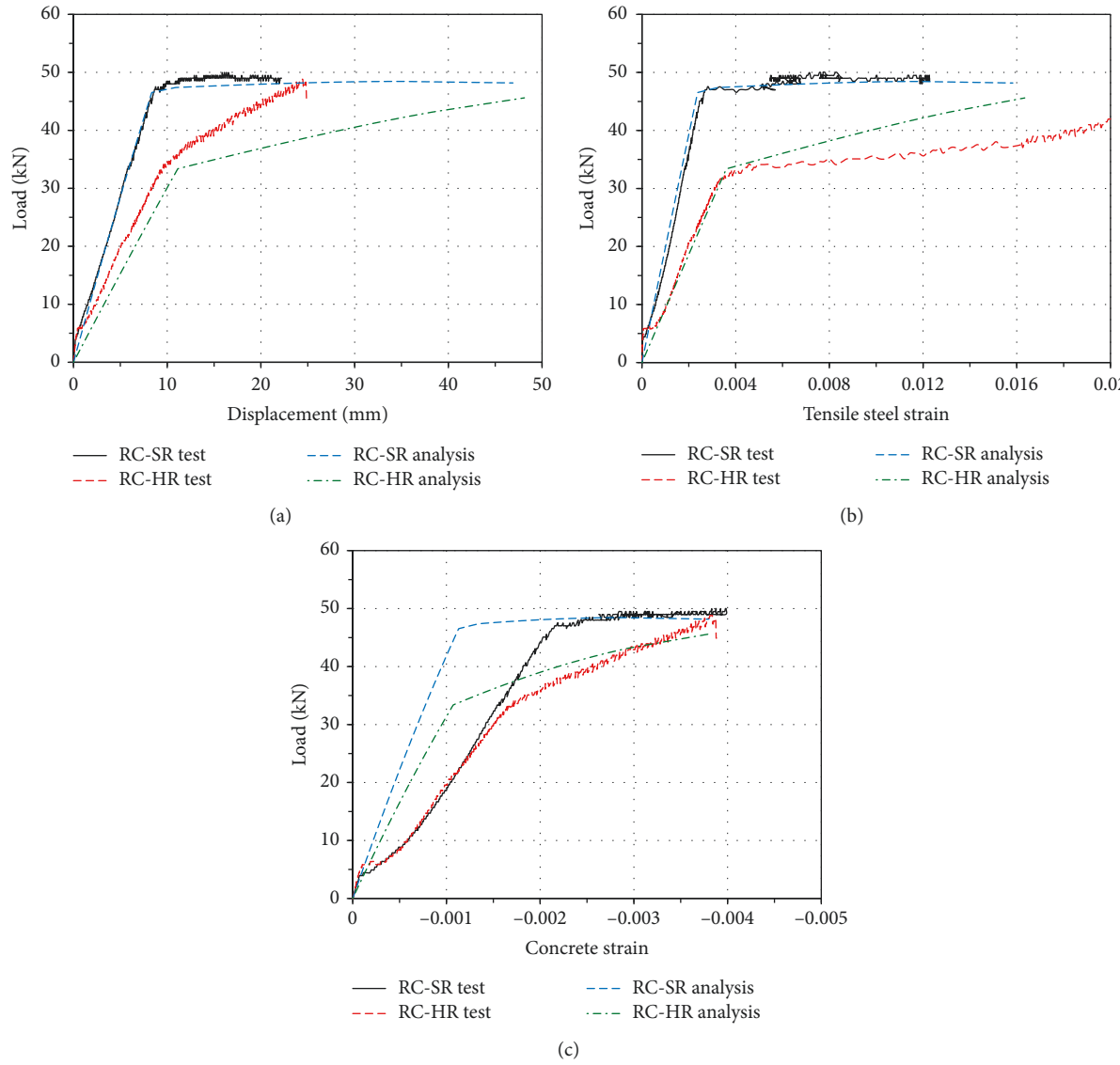

Figure 13: Comparison of predicted and experimental static flexural behaviors of RC beam specimens reinforced by the steel rebar (RC-SR) and by the hybrid FRP-steel rebar (RC-HR): (a) load-deflection curves at midspan; (b) load-tensile strain curves in longitudinal reinforcement; (c) load-concrete compressive strain curves.

6.2. Fatigue Behavior. Figures 14 and 15 compare the predicted and experimental fatigue behaviors of the considered RC beam specimens RC-SR and RC-HR, respectively. The predicted fatigue behavior is obtained by the process depicted in Figure 12. In the graphs, the curves of the analytical results are drawn by linking the peak values for clarity purpose. The experimental values are those presented in Figure 9 of Section 3.2. Recall that the fatigue test was conducted 100 times after the yield of the longitudinal reinforcement and was followed by static loading until failure.

The fatigue test involved 100 loading cycles after yielding of the rebar followed by static loading to failure. Besides, the fatigue analysis applied only cyclic loading until failure. Considering that the test results plotted in Figures 14 and 15 represent those obtained under 100 loading cycles after yielding of the rebar followed by static loading to failure, these results differ naturally from the fatigue analysis conducted in this study. Moreover, even if the beam specimens were fabricated at once using the same materials and processes, the static test members differ from those for the fatigue test and include some fabrication error inherent to the characteristics of concrete.

Consequently, the analytical and experimental results cannot be compared beyond the point at which cyclic loading was interrupted. If we limit the comparison of the analytical and experimental results to the cyclic loading portion, the difference between the predicted and actual behaviors of RC-SR observed at the early loading can be simply attributed to the fact that these members are different to some extent and the existence of the fabrication error in the concrete members. In addition, there is also the error brought by the adopted analysis model as explained in the discussion on the static test results.

Nevertheless, the method simulating the low-cycle behavior of the reinforced concrete beam is found to provide

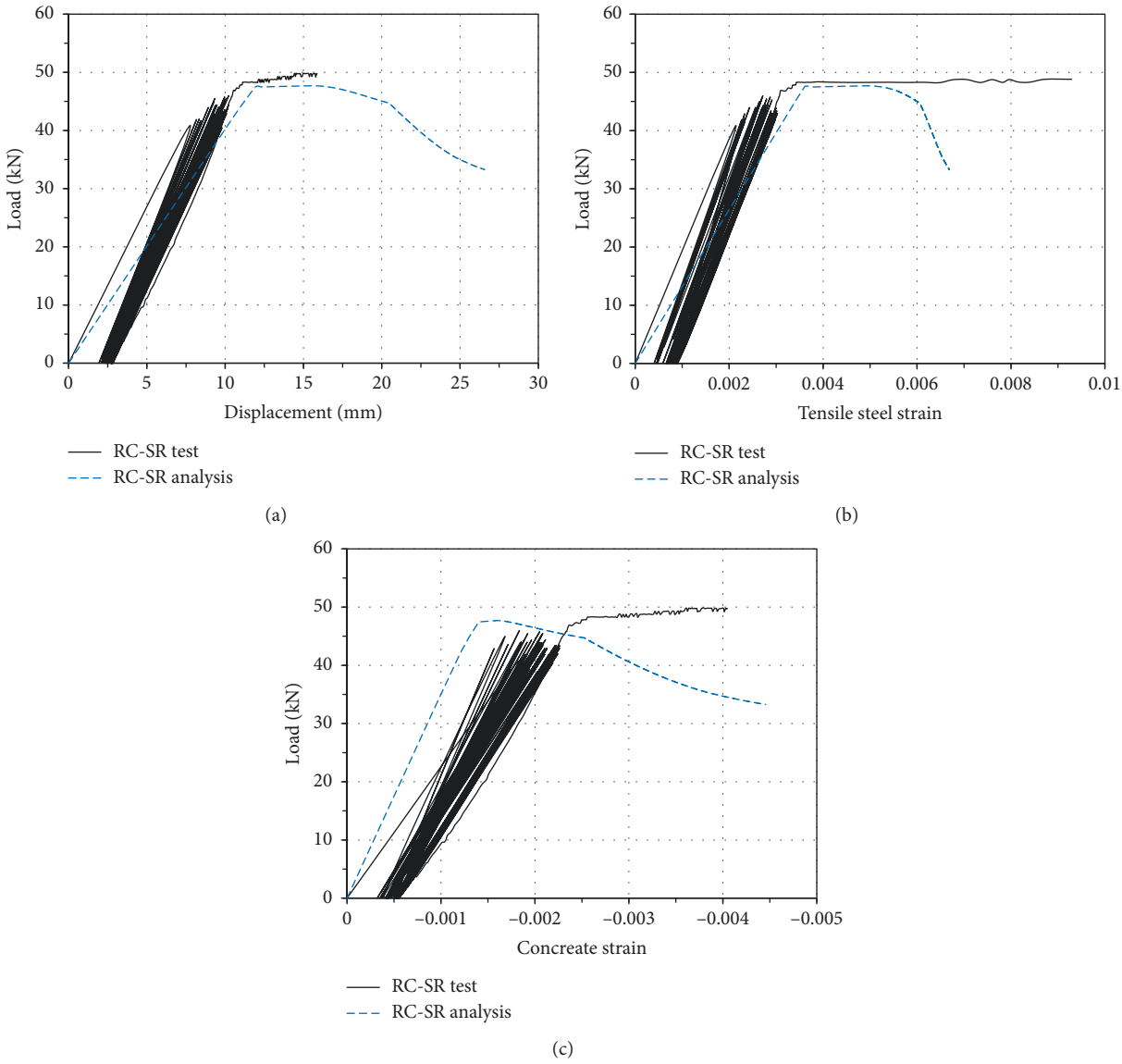

Figure 14: Comparison of predicted and experimental fatigue test results of RC-SR: (a) fatigue load-deflection curves at midspan of RC-SR; (b) fatigue load-tensile strain curves in longitudinal reinforcement of RC-SR; (c) fatigue load-concrete compressive strain curves of RC-SR.

results in good agreement with the experimental results. The larger difference exhibited for RC-HR can be attributed to the fact that the formula predicting the postyielding fatigue strain of the rebar in Equation (1) was formulated based upon the results of both steel and hybrid rebars with a higher correlation coefficient for the steel rebar and also to the fact that the steel rebar is of homogeneous nature, whereas the hybrid FRP-steel rebar gathers two materials different in nature and behavior. As arranged in Table 4, the analysis predicted the number of cycles to failure to be 7,670 cycles for RC-SR and 8,497 cycles for RC-HR. Moreover, all the RC beams were predicted to fail through compressive failure of concrete.

7. Conclusions

The hybrid FRP-steel bar was proposed as one solution to solve this problem, and numerous studies reported that the hybrid FRP-steel bar developed superior resistance to chloride attack than the conventional steel. The flexural behavior of the concrete beam reinforced with the hybrid FRP-steel rebar was mainly studied experimentally. However, there is still limited analytical research for predicting the performance of such RC beams under fatigue loading to enable them to be used safely on field. Accordingly, the present study proposed an analytical model predicting the low-cycle flexural fatigue behavior of the concrete beam reinforced with the hybrid FRP-steel bar. RC beam specimens reinforced with the hybrid FRP-steel rebar and conventional steel rebar were fabricated and subjected to the static test up to failure and the fatigue test at the low cycle up to 100 cycles after yielding of the longitudinal rebar.

The test results showed that the beam reinforced with the hybrid rebar exhibited better restoring force than the beam

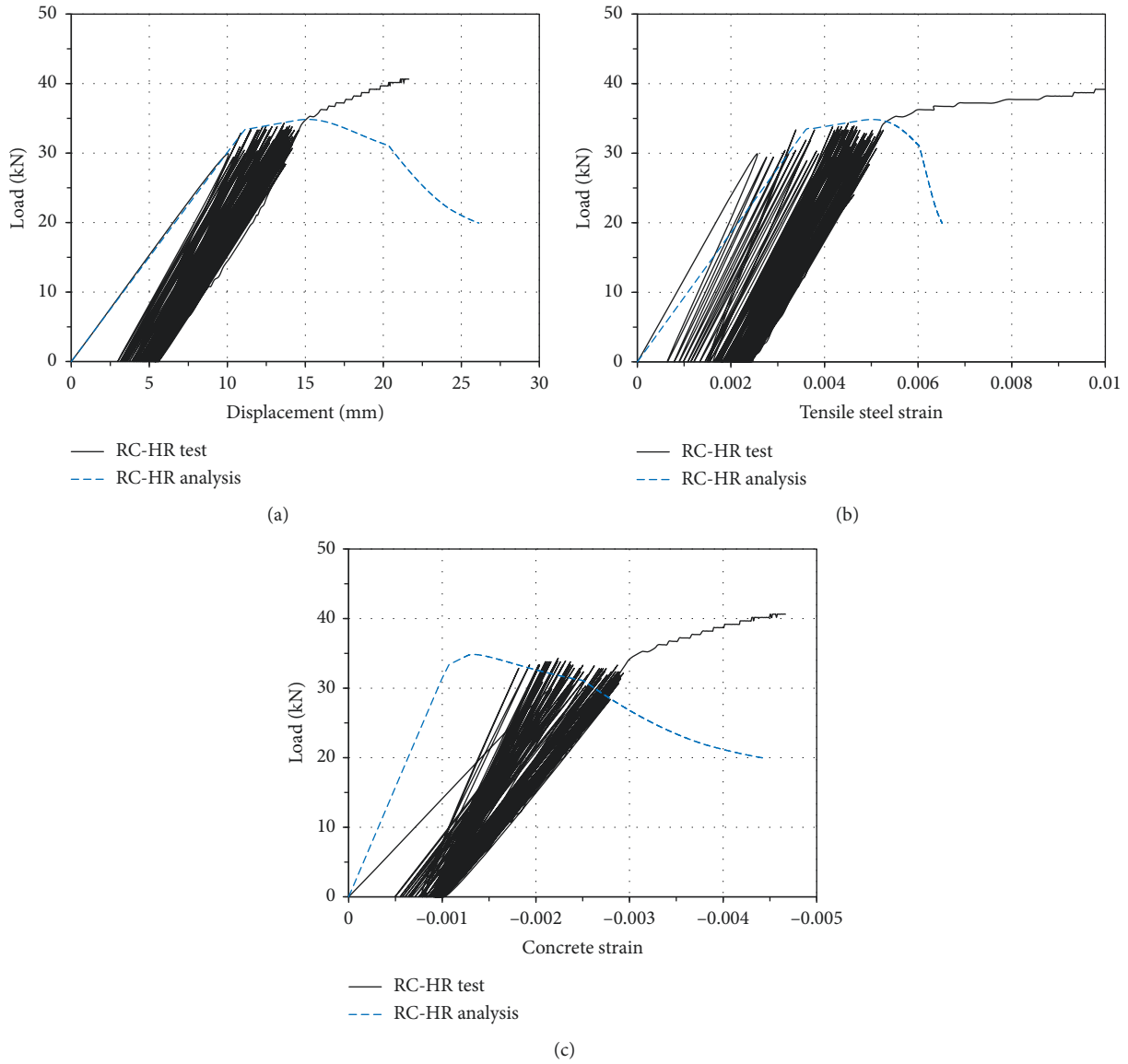

Figure 15: Comparison of predicted and experimental fatigue test results of RC-HR: (a) fatigue load-deflection curves at midspan of RC-HR; (b) fatigue load-tensile strain curves in longitudinal reinforcement of RC-HR; (c) fatigue load-concrete compressive strain curves of RC-HR.

Table 4: Results of fatigue analysis.

RC beam specimen	Number of cycles (N)	Failure pattern
RC-SR	7,670	Compressive failure of concrete
RC-HR	8,497	Compressive failure of concrete

reinforced with the steel rebar. In addition, the hybrid rebar developed postyielding tension hardening, which allowed the beam to behave linearly under larger load as reported in other studies. These results were used to establish a general formula relating the postyielding fatigue strain of the rebar to the number of the fatigue cycle regardless of the type of the rebar. An analytical procedure was then proposed using the so-established formula and based upon the strain compatibility condition to predict the low-cycle flexural fatigue behavior of the concrete beam reinforced with the steel rebar or hybrid FRP-steel bar. The analytical results revealed that the proposed approach could simulate satisfactorily the low-cycle fatigue behavior of the RC beams and predict the number of cyclic loading to failure. More accurate analytical results can be obtained by using a formula relating the postyielding fatigue strain of the rebar to the number of the fatigue cycle for one specific type of the rebar. However, the present study focused on the development of a general methodology simulating the low-cycle flexural fatigue behavior of RC beams.

Despite of its relatively long history and its clear merits, the hybrid rebar is still not applied on field due to numerous causes. The absence of the model predicting its fatigue behavior in a long term seems to be one of these causes. Since very long time would be required to observe experimentally the low-cycle fatigue behavior of the concrete beam reinforced with the hybrid FRP-steel rebar, the development of a realistic model enabling to predict such behavior and the potential lifespan of the structure under cyclic loading is meaningful. Therefore, the authors believe that the proposed model and methodology will fill this gap and contribute to the field application of such reinforced concrete beams.

Data Availability

The data used to support the findings of this study are available from the corresponding author upon request.

Conflicts of Interest

The authors declare that they have no conflicts of interest.

Acknowledgments

This research was financially supported by the Korean Ministry of Environment as "Public Technology Program Based on Environmental Policy" (2016000700003). And this research was also financially supported by the Technology Advancement Research Program (TARP) (Grant no. 18CTAP-C129778-02) funded by the Ministry of Land, Infrastructure and Transport of the Korean government.

References

[1] L. Chung, J. H. J. Kim, and S. T. Yi, "Bond strength prediction for reinforced concrete members with highly corroded reinforcing bars," *Cement and Concrete Composites*, vol. 30, no. 7, pp. 603–611, 2008.

[2] H. Yalciner, O. Eren, and S. Sensoy, "An experimental study on the bond strength between reinforcement bars and concrete as a function of concrete cover, strength and corrosion level," *Cement and Concrete Research*, vol. 42, no. 5, pp. 643–655, 2012.

[3] F. Tondolo, "Bond behaviour with reinforcement corrosion," *Construction and Building Materials*, vol. 93, pp. 926–932, 2015.

[4] L. Wang, C. Li, and J. Yi, "An experiment study on behavior of corrosion RC beams with different concrete strength," *Journal of Coastal Research*, vol. 73, pp. 259–264, 2015.

[5] A. Nanni, J. Nenninger, K. Ash, and J. Liu, "Experimental bond behavior of hybrid rods for concrete reinforcement," *Structural Engineering and Mechanics*, vol. 5, no. 4, pp. 339–354, 1997.

[6] F. Micelli and A. Nanni, "Durability of FRP rods for concrete structures," *Construction and Building Materials*, vol. 18, no. 7, pp. 491–503, 2004.

[7] T. Alkhrdaji, A. Nanni, G. Chen, and M. Barker, "Upgrading the transportation infrastructure: solid RC decks strengthened with FRP," *Concrete International: Design & Construction*, vol. 21, no. 10, pp. 37–41, 1999.

[8] F. Ceroni, E. Cosenza, M. Gaetano, and M. Pecce, "Durability issues of FRP rebars in reinforced concrete members," *Cement and Concrete Composites*, vol. 28, no. 10, pp. 857–868, 2006.

[9] H. G. Harris, W. Somboonsong, and F. K. Ko, "New ductile hybrid FRP reinforcing bar for concrete structures," *Journal of Composites for Construction*, vol. 2, no. 1, pp. 28–37, 1998.

[10] B. Saikia, J. Thomas, A. Ramaswamy, and K. S. Nanjunda Rao, "Performance of hybrid rebars as longitudinal reinforcement in normal strength concrete," *Materials and Structures*, vol. 38, pp. 857–864, 2005.

[11] D. W. Seo, K. T. Park, Y. J. You, and J. H. Hwang, "Evaluation for tensile performance of recently developed FRP hybrid bars," *International Journal of Emerging Technology and Advanced Engineering*, vol. 4, no. 6, pp. 631–637, 2014.

[12] D. W. Seo, K. T. Park, Y. J. You, and S. Y. Lee, "Experimental investigation for tensile performance of GFRP-steel hybridized rebar," *Advances in Materials Science and Engineering*, vol. 2016, Article ID 9401427, 12 pages, 2016.

[13] J. P. Won and C. G. Park, "Effect of environmental exposure on the mechanical and bonding properties of hybrid FRP reinforcing bars for concrete structures," *Journal of Composite Materials*, vol. 40, no. 12, pp. 1063–1076, 2016.

[14] S. A. A. Mustafa and H. A. Hassan, "Behavior of concrete beams reinforced with hybrid steel and FRP composites," *HBRC Journal*, 2017, In press.

[15] I. F. Kara, A. F. Ashour, and M. A. Köroğlu, "Flexural behavior of hybrid FRP/steel reinforced concrete beams," *Composite Structures*, vol. 129, pp. 111–121, 2015.

[16] Z. Sun, Y. Tang, Y. Luo, G. Wu, and X. He, "Mechanical properties of steel-FRP composite bars under tensile and compressive loading," *International Journal of Polymer Science*, vol. 2017, Article ID 5691278, 11 pages, 2017.

[17] H. Y. Zhou, Y. B. Chen, J. C. Ci, and C. K. Yang, "Research status of fatigue damage mechanism of reinforced concrete beam," *Applied Mechanics and Materials*, vol. 858, pp. 44–49, 2016.

[18] J. H. Xie, P. Y. Huang, and Y. C. Guo, "Fatigue behavior of reinforced concrete beams strengthened with prestressed fiber reinforced polymer," *Construction and Building Materials*, vol. 27, no. 1, pp. 149–157, 2012.

[19] D. Li, P. Huang, G. Qin, X. Zheng, and X. Guo, "Fatigue crack propagation behavior of RC beams strengthened with CFRP under high temperature and high humidity environment," *International Journal of Polymer Science*, vol. 2017, Article ID 1247949, 11 pages, 2017.

[20] R. Al-Hammoud, K. Soudki, and T. H. Topper, "Fatigue flexural behaviour of corroded reinforced concrete beams repaired with CFRP sheets," *Journal of Composites for Construction*, vol. 15, no. 1, pp. 42–51, 2011.

[21] L. Song and Z. Yu, "Fatigue performance of corroded reinforced beams strengthened with CFRP sheets," *Construction and Building Materials*, vol. 90, pp. 99–109, 2015.

[22] H. G. Harris, F. P. Hampton, S. Martin, and F. K. Ko, "Cyclic behavior of a second generation ductile hybrid fiber reinforced polymer (D-H-FRP) for earthquake resistant concrete structures," in *Proceedings of 12th World Conference on Earthquake Engineering*, p. 8, Auckland, New Zealand, January 2000.

[23] J. P. Won, C. G. Park, S. J. Lee, and B. T. Hong, "Durability of hybrid FRP reinforcing bars in concrete structures exposed to marine environments," *International Journal of Structural Engineering*, vol. 4, no. 1-2, pp. 63–74, 2013.

[24] J. S. Sim, H. W. Kwon, H. H. Lee, and T. S. Kang, "An experimental study for bending characteristic of concrete beam

reinforced with FRP rebar under fatigue," *Journal of Engineering and Technology*, vol. 20, pp. 31–38, 2010, in Korean.
[25] C. S. Hwang, J. S. Park, K. T. Park, and S. J. Kwon, "Mechanical performance evaluation of RC beams with FRP hybrid bars under cyclic load," *Journal of the Korea institute for Structural Maintenance Inspection*, vol. 21, no. 1, pp. 9–14, 2017, in Korean.
[26] E. Hognestad, "Ultimate strength of reinforced concrete in American design practice," in *Proceedings of Symposium on the Strength of Concrete Structures*, London, UK, May 1956.
[27] S. W. Yoo, G. S. Ryu, and J. F. Choo, "Evaluation of the effects of high-volume fly ash on the flexural behavior of reinforced concrete beams," *Construction and Building Materials*, vol. 93, pp. 1132–1144, 2015.